



	Experiment title: Enhancing the Magnetic Order in Cr-doped Sb ₂ Te ₃ Topological Insulator Thin Films	Experiment number: HC-2718
Beamline: ID32	Date of experiment: from: 10 Nov 2016 to: 14 Nov 2016	Date of report: 1 March 2017
Shifts: 12	Local contact(s): K. Kummer	<i>Received at ESRF:</i>
Names and affiliations of applicants (* indicates experimentalists): L. B. Duffy (University of Oxford)* L. Gladczuk (University of Oxford)* T. Hesjedal (University of Oxford)* N.-J. Steinke (ISIS)* A. I. Figueroa (Diamond Light Source)* G. van der Laan (Diamond Light Source)*		

Report: see next page

Enhancing the Magnetic Order in Cr-doped Sb_2Te_3 Topological Insulator Thin Films

L. B. Duffy,^{1,2} A. I. Figueroa,³ L. Gładczuk,^{1,3} N.-J. Steinke,² K. Kummer,⁴ G. van der Laan,³ and T. Hesjedal¹

¹*Department of Physics, Clarendon Laboratory, University of Oxford, Oxford, OX1 3PU, United Kingdom*

²*ISIS, STFC, Rutherford Appleton Lab, Didcot, OX11 0QX, United Kingdom*

³*Magnetic Spectroscopy Group, Diamond Light Source, Didcot, OX11 0DE, United Kingdom*

⁴*European Synchrotron Radiation Facility, BP 220, 38043 Grenoble Cedex, France*

(Dated: March 5, 2017)

In our ESRF experiment HC-2718 we performed x-ray absorption spectroscopy measurements at the Cr $L_{2,3}$ edges on *in-situ* cleaved Cr-doped Sb_2Te_3 samples. Surface-sensitive x-ray magnetic circular dichroism was studied as a function of applied magnetic field and temperature to produce Arrott plots, which gave a T_C of the cleaved film of ~ 87 K. Through *in-situ* evaporation of Co, the transition temperature measured at the surface of the $\text{Cr}_{0.3}\text{Sb}_{1.7}\text{Te}_3$ films increased to T_C to ~ 93 K. A clean interface between the magnetically doped TI and the deposited ferromagnetic thin film of Co is demonstrated via spectroscopic analysis.

I. INTRODUCTION

Topological insulators (TIs) are of key significance due to their exotic physical nature and promising electronic properties,^{1,2} which could lead to advancements in low-power consumption devices for a range of applications.³ Three-dimensional TIs have gapless topological surface states protected by time-reversal symmetry (TRS), which take the form of linearly dispersed Dirac cones with spin-momentum locking.⁴ These states are resilient to weak disorder or impurities,⁵ however, by breaking the TRS a gap can be opened at the Dirac point. This has led to both the prediction and observation of exotic quantum phenomena. Most notably the quantum anomalous Hall effect (QAHE), a fundamental quantum transport phenomenon, has been observed which may be the key to unlock major advancements in dissipationless quantum electronics.⁶ The breaking of TRS can be achieved either by applying a magnetic field, via the proximity to a ferromagnetic layer, or by achieving magnetic long-range order in the TIs by doping with, e.g., Fe,⁷ Mn,⁸ or Cr.⁹ Magnetically doped TIs have shown a giant spin-orbit torque, tunable via the use of an electric field, demonstrating potential applications for spintronics.¹⁰

In ESRF experiment HC-2718, we investigate the magnetic properties of *in-situ* cleaved $\text{Cr}_{0.3}\text{Sb}_{1.7}\text{Te}_3$ thin films using x-ray magnetic circular dichroism (XMCD). The isothermal magnetization is measured using XMCD as a function of field in order to produce Arrott plots,¹¹ which reveal a T_C of ~ 87 K — similar to a value previously measured in bulk-sensitive measurements.¹² When evaporating a thin Co film onto the cleaved surface at low temperatures, a clean interface between the two layers is confirmed through the comparison between the XMCD signal at the Cr-edge before and after the deposition. The transition temperature of the surface of the $\text{Cr}_{0.3}\text{Sb}_{1.7}\text{Te}_3$ film is enhanced by the Co layer through the proximity effect to ~ 93 K. This demonstrates that unlike other systems, the proximity-effect between the Co layer and magnetically doped TI layer is weaker than expected.

II. EXPERIMENTAL

Molecular-beam epitaxy (MBE) was used to grow Cr-doped Sb_2Te_3 thin films on *c*-plane sapphire substrates. The typical film thickness was ~ 40 nm. For the Sb_2Te_3 growth, a Sb:Te flux ratio of 1:10 was maintained. Cr was provided out of a high-temperature effusion cell, while maintaining a flux ratio of (Sb+Cr):Te of 1:10. The thin film deposition took place at a substrate temperature of 250°C . A detailed description of the growth procedure can be found in Ref. 12.

Structural and magnetic characterization was carried out using x-ray diffraction (XRD) and SQUID magnetometry, respectively and these measurements are also found in Ref. 12. Out-of-plane XRD measurements show that the films are free from secondary phases, such as chromium tellurides. The results are also consistent with Cr is substituting for Sb through the shift of Sb_2Te_3 peak positions to higher angles. This is due to a reduction in the Cr-Te bond length, when compared to the Sb-Te bonds, since Cr has a smaller ionic radius.¹² SQUID magnetometry demonstrates the samples are ferromagnetic, with a coercive field of ~ 50 mT at 5 K, and with an out-of-plane easy axis (saturation field is 200 mT) and an in-plane hard axis (saturation field is 2 T). The T_C of the film, defined by the minimum of the first derivative of the temperature-dependent magnetization,¹² is ~ 72 K.

XMCD measurements were performed on beamline ID32 at the European Synchrotron Radiation Facility (ESRF) in Grenoble. X-ray absorption spectroscopy (XAS) was measured at the Co and Cr $L_{2,3}$ edges in total-electron-yield mode (TEY), giving a surface sensitive probing depth of 3-5 nm.¹³ The samples were cleaved in ultrahigh vacuum to ensure a pristine surface. The XMCD was obtained by taking the difference between recorded XAS spectra with the helicity vector parallel and antiparallel to the applied magnetic field, respectively. The measurements were done with the sample both normal to the incident x rays and at an angle of 54.7° to accommodate for the perpendicular magnetization directions of the Co and the TI.¹⁴ After perform-

ing measurements on the pristine sample, Co was evaporated from an e-beam evaporator situated inside the XAS measurement chamber (base pressure $<1 \times 10^{-9}$ Torr) at a temperature <10 K. This low-temperature evaporation prevents clustering of the Co atoms.¹⁵ To ensure the thickness of the Co layer was ≥ 3 nm, XAS measurements were carried out periodically after different stages of evaporation. Both the XAS and XMCD lineshape and intensity were observed during this process at both the Co and Cr $L_{2,3}$ edges to ensure they remained consistent with clean Cr and a previously grown clean 3-nm thick Co film.

III. RESULTS

Figure 1 shows the Cr $L_{2,3}$ XAS and XMCD measured in TEY for the cleaved $\text{Cr}_{0.3}\text{Sb}_{1.7}\text{Te}_3$ sample. The main Cr peak is consistent with a divalent state as reported for $\text{Cr}:\text{Bi}_2\text{Se}_3$ in Ref. 16, suggesting that the Cr goes substitutionally onto the Sb sites. The absence of an extra peak structure at 577.5 eV in both the XAS and XMCD, confirms the absence of trivalent Cr otherwise found in an oxidized surface layer.

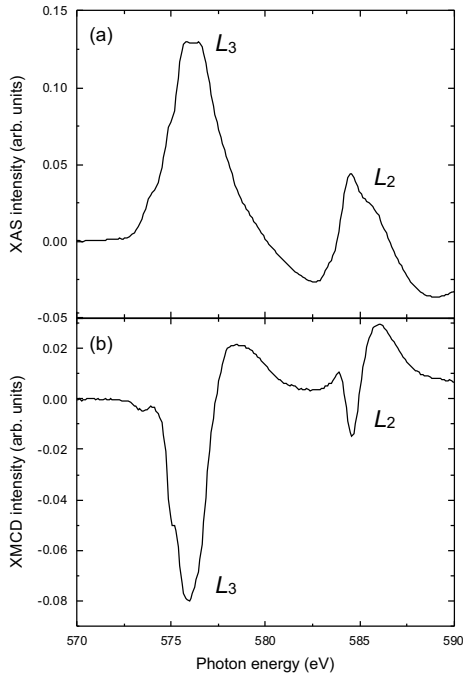


FIG. 1. (a) XAS and (b) XMCD of *in-situ* cleaved $\text{Cr}_{0.3}\text{Sb}_{0.7}\text{Te}_3$ film measured at the Cr $L_{2,3}$ edges in zero field at 10 K, and at normal incidence of the incident x-rays. The lineshapes for the XAS and XMCD are consistent with nominal Cr^{2+} , as expected for substitutional Cr doping on Sb sites.

Figure 2(a) shows the XAS and XMCD spectra obtained from the cleaved $\text{Cr}:\text{Sb}_2\text{Te}_3$ sample after Co de-

position. Analysis of the spectra for the Co peak demonstrates that there is no interfacial reaction between the TI and the ferromagnetic layer. Figure 2(b) demonstrates that the Cr XMCD is unaffected by the Co deposition, which suggests that the chemical state of Cr in the TI remains the same.

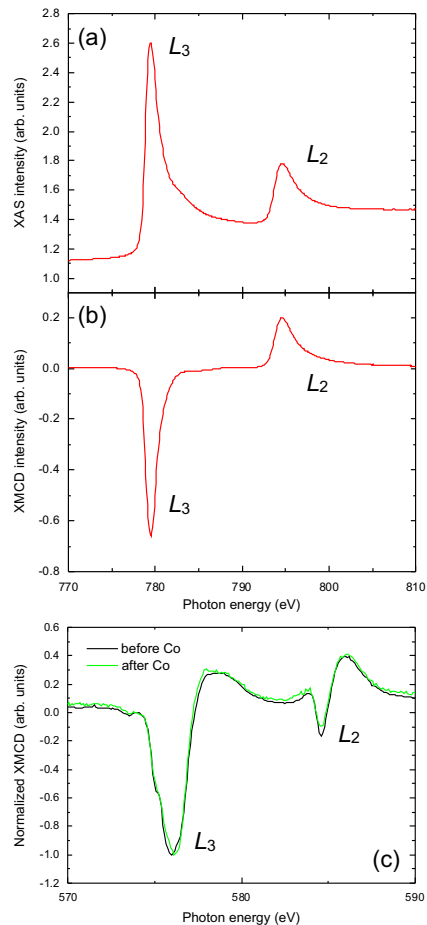


FIG. 2. (a) XAS and (b) XMCD of an *in-situ* cleaved $\text{Cr}:\text{Sb}_2\text{Te}_3$ film after Co deposition measured at the Co $L_{2,3}$ edge in an applied magnetic field of 8 T and a temperature of 10 K. The incident angle of the x-rays was 54° . Both the XAS and XMCD signals are strong, demonstrating the magnetic quality of the deposited Co. (c) Comparison of the Cr $L_{2,3}$ XMCD signals before (black line) and after (green line) Co deposition. Note that the lineshapes are identical, demonstrating that Co is not affecting the chemical or magnetic properties of Cr.

The most reliable method for determining the Curie temperature of a ferromagnet are Arrott plots, because this method minimizes the contribution arising from domain rotation and magnetic anisotropy. In the case of a conventional second-order ferromagnetic transition, Arrott plot should give positively sloped straight lines, if the magnetic field is high enough that possible domains or stray field effects become negligible. An Arrott plot is given by the isotherms of M^2 vs H/M , where M is the magnetization (as measured by XMCD), and H is the ap-

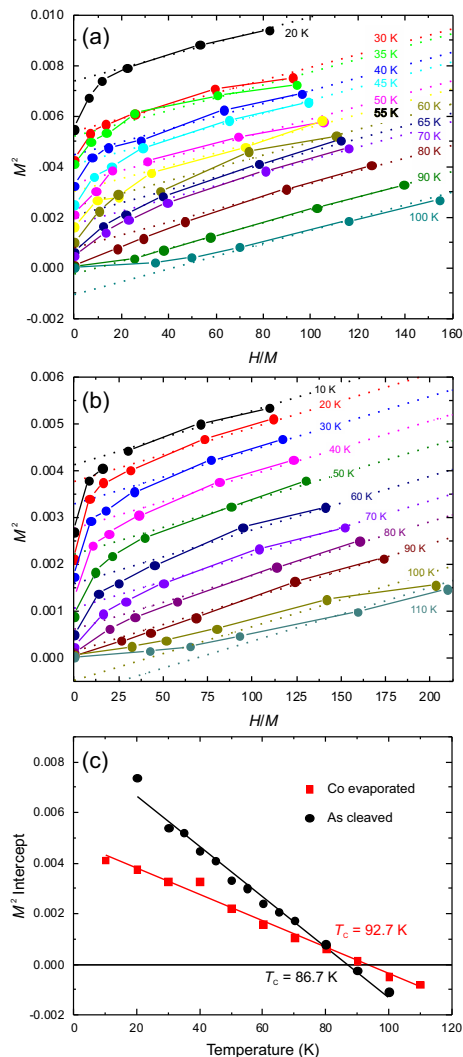


FIG. 3. Arrott plots for (a) the as-cleaved $\text{Cr}_0.3\text{Sb}_{1.7}\text{Te}_3$ sample and (b) after Co deposition. The isothermal variations of M^2 are plotted as a function of H/M , where H is the applied field and M is the magnetization as measured by the XMCD asymmetry of the Cr L_3 peak using TEY. In both cases, a straight line was fitted (shown as dotted lines) to the three data points obtained at the highest fields at each temperature. (c) M^2 intercepts obtained from (a) and (b) plotted against temperature. The straight lines are guides to the eye. The temperature at which M^2 vanishes is defined as the Curie temperature. The values for the as cleaved (black) and Co decorated surfaces are 86.7 K and 92.7 K, respectively.

plied field. The intercept of the isotherms with H/M axis is positive for $T > T_C$ and negative for $T < T_C$. Hence, T_C is equal to that temperature for which the isotherm passes through the origin, i.e., the H/M intercept is zero.

Figure 3(a) shows the Arrott plot for the as-cleaved $\text{Cr}_0.3\text{Sb}_{1.7}\text{Te}_3$ sample generated using the background-corrected Cr L_3 XMCD asymmetry, which is directly proportional to M . Figure 3(b) shows Arrott plot produced in the same manner for the same sample with Co deposited onto the surface. The phase transition is of second order as the magnetization increases continuously for lower temperatures, which is expected of a ferromagnetic transition. Figure 3(c) shows the M^2 intercepts gathered by fitting parallel straight lines with the same gradient to the high-field regions of each isotherm. The zero crossing for the as-cleaved sample gives a $T_C \approx 87$ K. After the Co overlayer is deposited, the T_C rises to ~ 93 K, which is a rather modest increase.

These results will be submitted for publication.

- ¹ L. Fu, C. L. Kane, and E. J. Mele, *Phys. Rev. Lett.*, **98**, 106803 (2007).
- ² B. A. Bernevig, T. L. Hughes, and S.-C. Zhang, *Science*, **314**, 1757 (2006).
- ³ M. Z. Hasan and C. L. Kane, *Rev. Mod. Phys.*, **82**, 3045 (2010).
- ⁴ Y. L. Chen, J. G. Analytis, J.-H. Chu, Z. K. Liu, S.-K. Mo, X.-L. Qi, H. J. Zhang, D. H. Lu, X. Dai, Z. Fang, *et al.*,

Science, **325**, 178 (2009).

- ⁵ P. Roushan, J. Seo, C. V. Parker, Y. S. Hor, D. Hsieh, D. Qian, A. Richardella, M. Z. Hasan, R. J. Cava, and A. Yazdani, *Nature*, **460**, 1106 (2009).
- ⁶ S. Qi, Z. Qiao, X. Deng, E. D. Cubuk, H. Chen, W. Zhu, E. Kaxiras, S. B. Zhang, X. Xu, and Z. Zhang, *Phys. Rev. Lett.*, **117**, 056804 (2016).
- ⁷ Y. Okada, C. Dhital, W. Zhou, E. D. Huemiller, H. Lin,

- S. Basak, A. Bansil, Y.-B. Huang, H. Ding, Z. Wang, *et al.*, Phys. Rev. Lett., **106**, 206805 (2011).
- ⁸ L. J. Collins-McIntyre, M. D. Watson, A. A. Baker, S. L. Zhang, A. I. Coldea, S. E. Harrison, A. Pushp, A. J. Kellock, S. S. P. Parkin, G. van der Laan, *et al.*, AIP Advances, **4**, 127136 (2014).
- ⁹ L. J. Collins-McIntyre, S. E. Harrison, P. Schönherr, N.-J. Steinke, C. J. Kinane, T. R. Charlton, D. Alba-Veneroa, A. Pushp, A. J. Kellock, S. S. P. Parkin, *et al.*, Eur. Phys. Lett., **107**, 57009 (2014).
- ¹⁰ Y. Fan, X. Kou, P. Upadhyaya, Q. Shao, L. Pan, M. Lang, X. Che, J. Tang, M. Montazeri, K. Murata, *et al.*, Nat. Nanotechnol., **11**, 352 (2016).
- ¹¹ A. Arrott, Phys. Rev., **108**, 1394 (1957).
- ¹² L. J. Collins-McIntyre, L. B. Duffy, A. Singh, N.-J. Steinke, C. J. Kinane, T. R. Charlton, A. Pushp, A. J. Kellock, S. S. P. Parkin, S. N. Holmes, *et al.*, Eur. Phys. Lett., **115**, 27006 (2016).
- ¹³ G. van der Laan and A. I. Figueroa, Coord. Chem. Rev., **277**, 95 (2014).
- ¹⁴ G. van der Laan, B. T. Thole, G. A. Sawatzky, J. B. Goedkoop, J. C. Fuggle, J.-M. Esteve, R. Karnatak, J. P. Reimeika, and H. A. Dabkowska, Phys. Rev. B, **34**, 6529 (1986).
- ¹⁵ L. R. Shelford, T. Hesjedal, L. Collins-McIntyre, S. S. Dhesi, F. Maccherozzi, and G. van der Laan, Phys. Rev. B, **86**, 081304(R) (2012).
- ¹⁶ A. I. Figueroa, G. van der Laan, L. J. Collins-McIntyre, S.-L. Zhang, A. A. Baker, S. E. Harrison, P. Schönherr, G. Cibin, and T. Hesjedal, Phys. Rev. B, **90**, 134402 (2014).